ChemPubSoc Europe

DOI: 10.1002/ejoc.202000035

EurJOC European Journal of Organic Chemistry

Full Paper

Optical Resolution | *Very Important Paper* |

Scalable Enantiomeric Separation of Dialkyl-Arylphosphine Oxides Based on Host–Guest Complexation with TADDOL-Derivatives, and their Recovery

Bence Varga,[a] Réka Herbay,[a] György Székely,[b,c] Tamás Holczbauer,[d] János Madarász,[e] Béla Mátravölgyi,[a] Elemér Fogassy,[a] György Keglevich,[a] and Péter Bagi*[a]

Abstract: Several dialkyl-arylphosphine oxides were prepared, and the enantioseparation of the corresponding racemates was elaborated with host–guest complexation using TADDOL-derivatives. The crystallization conditions were optimized and two separate crystallization methods, one in organic solvent, and the other in water, were found to yield five examples of phosphine oxides with enantiomeric excess values higher than 94 %. A gram scale resolution was performed, and both enantiomers of the methyl-phenyl-propyl-phosphine oxide were separated with (*R*,*R*)- or (*S*,*S*)-spiro-TADDOL. The intermolecular interactions responsible for the enantiomeric recognition between the chiral host and guest molecules were investigated by single-crystal X-ray diffractional structural determinations. The similarities in the structural patterns of a few diastereomeric crystals were checked by powder X-ray diffraction, as well. Organic solvent nanofiltration (OSN) was used as a scalable technique for the decomposition of the corresponding phosphine oxide–spiro-TADDOL molecular complexes, and for the recovery of the phosphine oxide enantiomers and resolving agents.

Introduction

The chiral organophosphorus compounds, in particular the ones bearing a *P*-stereogenic center, form an interesting class, and the preparation of *P*-stereogenic enantiomers became an emerging area in the last decades.[1] Although many privileged *P*-ligands have been synthesized,[2] the number of chiral phosphines, phosphine oxides or phosphonium salts used as organocatalysts is constantly increasing.[3] Thus, the preparation of novel chiral organophosphorus scaffolds is still of great interest.

Among the methods developed for the preparation of *P*-stereogenic compounds, there is not a universal one, and every method has its own scope and limitations.[1,4] In these methods, the *P*-chiral compounds are usually prepared as bench stable phosphine boranes or oxides, and the air sensitive P^{III}-derivatives are liberated prior to the application.[1a,5] The methods developed for the preparation of *P*-stereogenic enantiomers include: stereoselective syntheses using chiral catalysts[6] bi-,[7] or monofunctional auxiliaries,[8] stereoselective transformation of >P(O)H species,[9] kinetic[10] or dynamic kinetic resolutions,[11] and classical resolutions (Figure 1).[12]

Several strategies require the manipulation with air- and moisture sensitive reagent(s) or intermediate(s), which makes these processes less suitable for scale up and industrial use. Many methods rely on the formation of covalent *P*-stereogenic intermediates with the usage of commercially available, but often expensive chiral auxiliaries.[7b–7e] However, the recycling of those chiral auxiliaries is sometimes neglected in those technologies,[8a–e,11f] or even involve the loss of the auxiliary as it is transformed into an unreactive derivative that cannot be reused.[11a,11c,11d]

The classical resolution of phosphine boranes or oxides is another alternative for the preparation of the corresponding *P*-stereogenic species in optically active form.

The optical resolution of phosphine oxides is a bench stable process, and the potential scalability, robustness and the recyclability of the resolving agents are the key advantages of such procedures. One drawback of the classical resolutions is

[a] *Department of Organic Chemistry and Technology, Budapest University of Technology and Economics*
Műegyetem rkp. 3., 1111 Budapest, Hungary
E-mail: pbagi@mail.bme.hu
[b] *Advanced Membranes and Porous Materials Center, Physical Science and Engineering Division (PSE), King Abdullah University of Science and Technology (KAUST)*
Thuwal, 23955–6900, Saudi Arabia
[c] *Department of Chemical Engineering and Analytical Science, The University of Manchester*
The Mill, Sackville Street, Manchester, M1 3BB, United Kingdom
[d] *Chemical Crystallography Research Laboratory and Institute of Organic Chemistry, Research Centre for Natural Sciences*
Magyar tudósok körútja 2., 1519 Budapest, Hungary
[e] *Department of Inorganic and Analytical Chemistry, Budapest University of Technology and Economics*
Szent Gellért tér 4., 1111 Budapest, Hungary
Supporting information and ORCID(s) from the author(s) for this article are available on the WWW under https://doi.org/10.1002/ejoc.202000035.

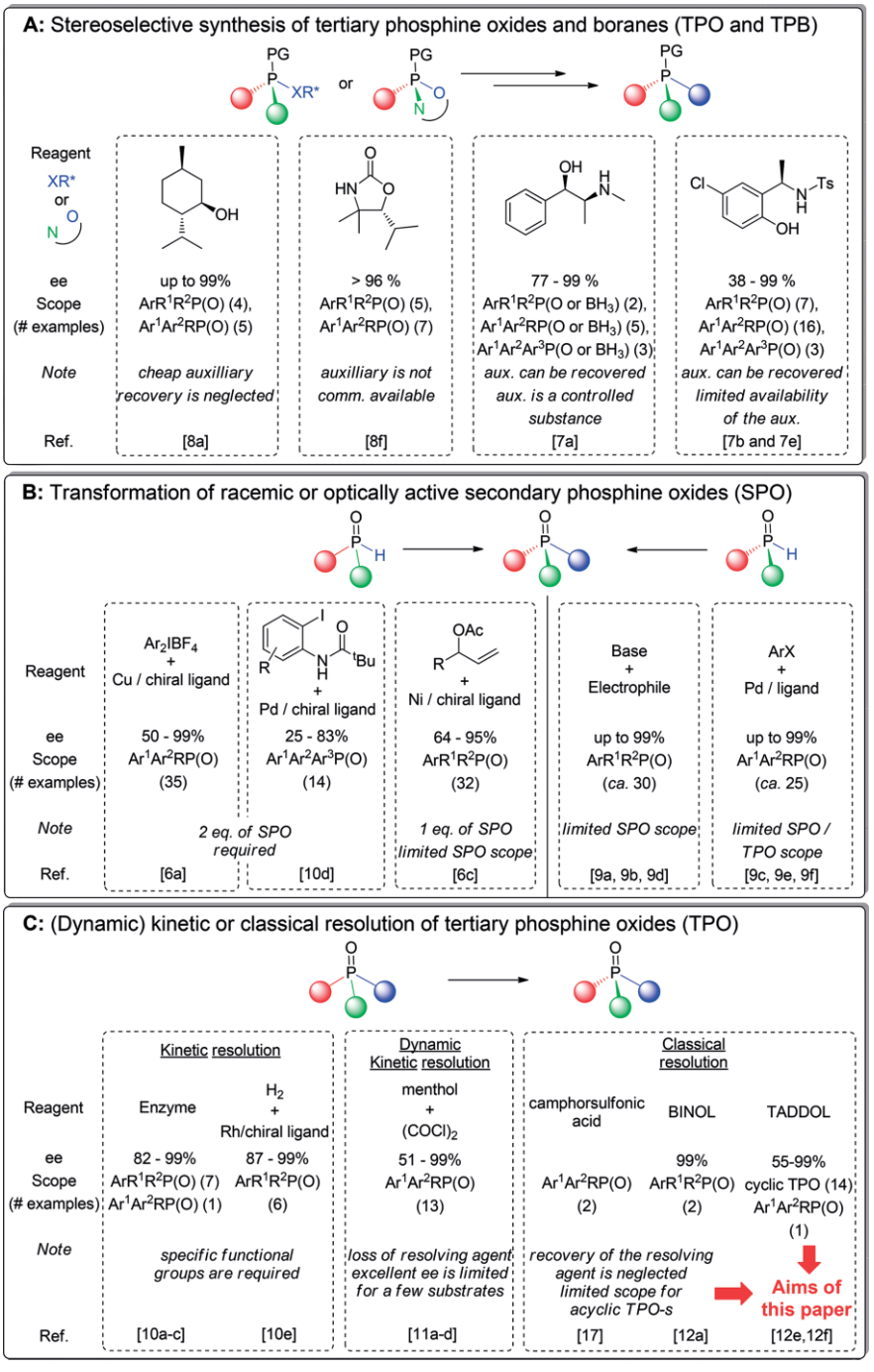

Figure 1. Selected examples showing the main strategies for the preparation of optically active tertiary phosphine oxides.

the 50 % limit in theoretical yield, which can be increased by the recycling and racemization of the undesired enantiomer.[12f,13] In general, resolution technologies utilize (relatively) inexpensive and commercially available acidic or basic resolving agents. In those instances, the ionic interactions are responsible for the enantiomeric recognition. The recovery of the pure enantiomer and the resolving agent can be accomplished by acid-base extractions, which are preferred in the industry.[14] However, the optical resolution becomes challenging for the non-acidic or non-basic racemates. For such substrates, the resolving agent classes capable of the formation of second order interactions (e.g. H-bonds, π–π interactions etc.) have great potential. BINOL- and TADDOL-type compounds meet the above mentioned criterion, and these resolving agent classes were used for the preparation of various enantiomers having neutral character based on host–guest complexations.[15] However, decomposition of the diastereomers, the recovery of the enantiopure product, and the recycling of the rather expensive resolving agents are the key challenges of such resolution procedures.[15c]

The optical resolution of *P*-stereogenic phosphine oxides may serve as a representative example of enantioseparations

based on host–guest complexation. The number of successful resolution methods for these organophosphorus compounds is limited.[16] A few commercially available chiral acids (e.g. camphorsulfonic acid, tartaric acid derivatives, mandelic acid) were applicable resolving agents, but those were rather individual examples with small scope, especially for secondary phosphine oxides.[12b–d,17] BINOL and the TADDOL derivatives were found to be efficient resolving agents for many cyclic and an acyclic *P*-stereogenic phosphine oxides.[12a,b,e,f] However, the scalable recovery of the phosphine oxide enantiomers and the resolving agents remained unresolved challenges of such resolution procedures. Distillation can be used for this separation, if the boiling point of the separated enantiomer is low, but column chromatography is used in most of the instances for the recovery of the enantiopure phosphine oxide and the resolving agent.[12e] However, the scalability of the column chromatography is limited. Separation of the enantiopure products and the resolving agents can be performed using organic solvent nanofiltration (OSN). OSN is a sustainable, pressure-driven membrane-based technology that is capable of distinguishing compounds between 50 and 2000 g mol^{-1} in organic media.[18] OSN processes developed for chiral molecules include enantioseparation,[19] asymmetric membrane reactor,[20] and continuous asymmetric catalyst recycling.[21]

In our earlier study, one optically active diaryl-alkylphosphine oxide was prepared, and those results suggested that TADDOL derivatives may be generally applicable resolving agents for acyclic phosphine oxides.[12f] Thus, the current study aims the enantioseparation of a series of dialkyl-arylphosphine oxides (**1–7**) by resolution based on host–guest complexation. The model phosphine oxides (**1–7**) incorporate one phenyl- and one methyl-group, which are common in most *P*-stereogenic ligands or organocatalysts.[2a,3c] Moreover, the methyl-group can be used for the construction of an ethylene bridge between two *P*-chiral centers.[22] Target phosphine oxides (**1–7**) are challenging, as the two alkyl groups may hinder the interactions between the chiral host and the guest molecules. This might be the reason why the literature lacks an efficient resolution method for dialkyl-arylphosphine oxides,[12a] and the stereoselective syntheses have their own scope and limitations.[7c,d,8c,d,9a,10e,23] TADDOL derivatives [(*R*,*R*)-**8**–(*R*,*R*,*R*,*R*)-**11**] were chosen for the resolution of these *P*-stereogenic dialkyl-arylphosphine oxides (**1–7**) (Figure 2.). The intermolecular interactions between the chiral host and guest molecules were investigated by single crystal or powder X-ray crystallography to gain some insight of the secondary interactions responsible for the enantiomeric recognition. The applicability of the OSN was also tested for the decomposition of the diastereomers, and for the recovery of the enantiomers and resolving agents.

Results and Discussion

Preparation of Racemic Dialkyl-Arylphosphine Oxides (1–7)

The methyl methylphenylphosphinate (**12a**) and ethyl ethylphenylphosphinate (**12b**) were used as starting materials in our

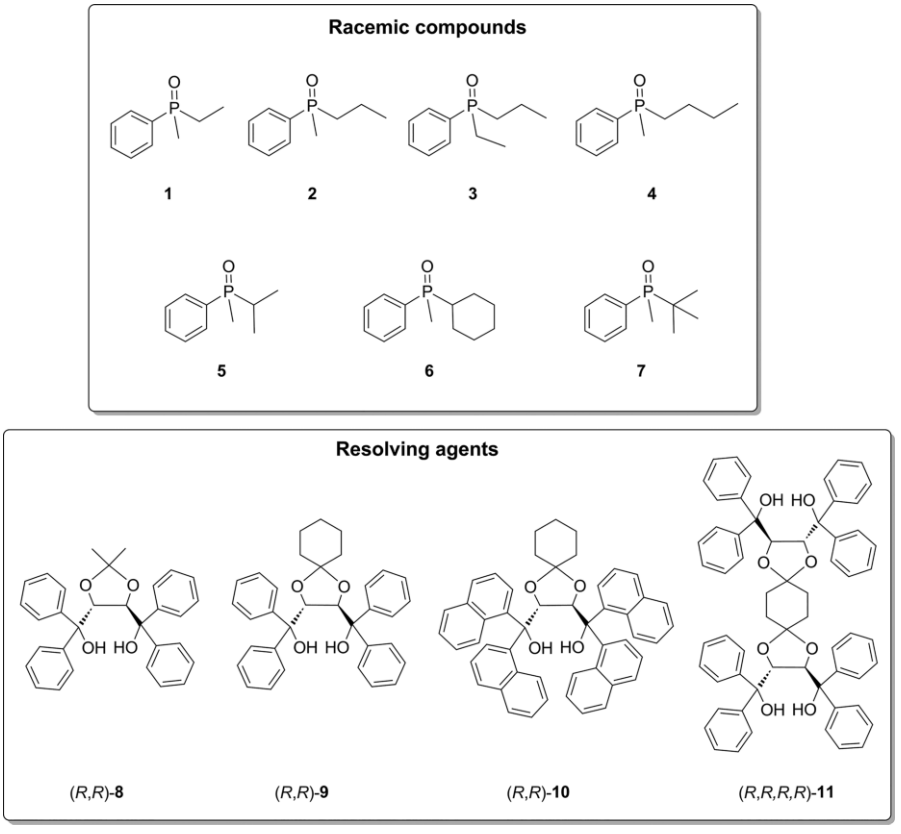

Figure 2. The racemic compounds (**1–7**) and the resolving agents [(*R*,*R*)-**8**–(*R*,*R*,*R*,*R*)-**11**] used in this study.

procedure. The corresponding phosphinates (**12**) were treated with the excess of the *Grignard*-reagent to give phosphine oxides (**1–6**) (Scheme 1). The advantage of this method is that it directly transforms the phosphinates (**12**) to the corresponding phosphine oxides (**1–6**) without the formation of the phosphinic chloride intermediates.[11a] The reactions with ethyl-, propyl- and butyl-magnesium bromides gave the phosphine oxides (**1–4**) in yields of 62–88 %. However, the reaction of methyl methylphenylphosphinate (**12a**) with *i*PrMgBr or *c*-HexMgBr afforded the corresponding phosphine oxides (**5** and **6**) with rather diminished yields (36 % and 35 %, respectively), which may be attributed to the increased steric bulk, and the higher basicity of the *Grignard*-reagents causing side reactions.

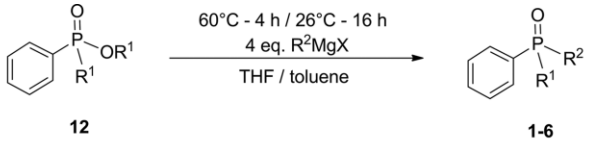

12 **1-6**

R^1 = Me (**a**) or Et (**b**)

Phosphine oxide	1	2	3	4	5	6
R^1	Me	Me	Et	Me	Me	Me
R^2	Et	Pr	Pr	Bu	*i*-Pr	*c*-Hex
Yield (%)	76	62	80	88	36	35

Scheme 1. Preparation of racemic phosphine oxides (**1–6**).

In order to prepare the *tert*-butyl-methyl-phenyl-phosphine oxide (**7**) phenylphosphonic dichloride (**13**) was treated with *t*Bu-MgCl and Me-MgCl in consecutive reactions. The phosphine so obtained was oxidized by H_2O_2 to give *tert*-butylmethylphenylphosphine oxide (**7**) in a yield of 67 % (Scheme 2). The *tert*-butylmethylphenylphosphine oxide (**7**) could not be prepared by the reaction of methyl methylphenylphosphinate (**12a**) with *t*Bu-MgCl due to the increased steric bulk of the organometallic reagent.

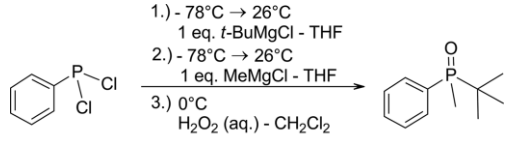

13 **7**

Scheme 2. Preparation of *tert*-butyl-methyl-phenyl-phosphine oxide (**7**).

Resolution of Methylphenylpropylphosphine Oxide (2) with TADDOL Derivatives [(*R*,*R*)-8–(*R*,*R*,*R*,*R*)-11]

The methylphenylpropylphosphine oxide (**2**) and spiro-TADDOL [(*R*,*R*)-**9**] were considered as model compounds, for our optimization study, as they both have "average" size within the scope of racemic compounds (**1–7**) and resolving agents [(*R*,*R*)-**8**–(*R*,*R*,*R*,*R*)-**11**] used (Scheme 3).

In our experiments, the racemic compound (**2**) and the resolving agent [(*R*,*R*)-**9**] were dissolved in the corresponding hot solvent, and the diastereomeric complexes appeared upon cooling, or by the addition of a co-solvent. In our preliminary studies, the amount of resolving agent [(*R*,*R*)-**9**] was adjusted to perform the resolutions according to the half-equivalent method. The temperature of the crystallization was set to 25 °C, and the crystallization time was 3 h. The crystalline intermediates separated by filtration were purified by additional crystallization(s).

A series of solvents and solvent mixtures were tested (See Supporting Information for the complete list of solvents). Interestingly, the enantiomeric selectivity of the spiro-TADDOL [(*R*,*R*)-**9**] was rather low in alcohols, despite the fact that these solvents were the most suitable ones in our previous studies (Table 1, Entry 1).[12e,12f] The results were improved when the diastereomers were precipitated by the addition of alkanes (hexane or heptane). A mixture of toluene and heptane was one of the most suitable medium affording the (*R*)-methylphenylpropylphosphine oxide [(*R*)-**2**] with an *ee* of 96 %, and in a yield of 25 % (Table 1, Entry 2). Other solvent mixtures, such as ethyl acetate and heptane or cymene and heptane led to low yield and *ee* values (Table 1, Entry 3; Supporting Information). A series of "green solvents", such as cymene, cyrene, cyclopentyl methyl ether, 2-Me-THF and ethyl lactate were also tested without success. The work of *Matsumoto* et al.[24] and *Tsunoda* et al.[25] prompted us to attempt the precipitation-mediated resolution in a mixture of methanol and water. To our delight, the (*R*)-methylphenylpropylphosphine oxide [(*R*)-**2**] was obtained with an *ee* of 80 %, and in a yield of 59 % after the first crystallization, and these results could be increased by recrystallization to afford (*R*)-**2** with an *ee* of 98 %, and in a yield of 48 %. Our efforts to improve these results with different molar ratios of spiro-TADDOL [(*R*,*R*)-**9**], ratios of MeOH and water, or with the applications of various alcohols failed (See Supporting Information for details). Moreover, a change in the reaction conditions often involved a change in the composition of the dia-

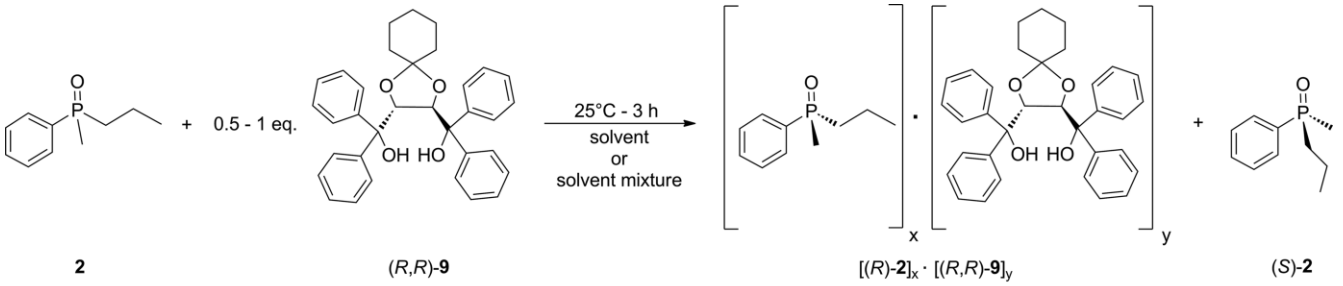

2 (*R*,*R*)-**9** [(*R*)-**2**]$_x$ · [(*R*,*R*)-**9**]$_y$ (*S*)-**2**

Precipitate *Solution*

Scheme 3. General procedure for the optimization of the resolution of methyl-phenyl-propyl-phosphine oxide (**2**) with spiro-TADDOL derivative [(*R*,*R*)-**9**].

Table 1. Resolution of methylphenylpropylphosphine oxide (**2**) with spiro-TADDOL [(*R*,*R*)-**9**].

Entry	Equiv. of (*R*,*R*)-**9**	Solvents[a]	Diastereomeric Complex[b]	Yield[c,f] (%)	*ee*[d,f] (%)	*S*[e,f] (–)	Abs. Config.[g]
1	1	6 × 2-PrOH	(**2**)•spiro-TADDOL$_2$	(64)	(35)	(0.22)	(*R*)
				20	**33**	**0.07**	
2	0.5	5 × toluene/5 × heptane	(**2**)•spiro-TADDOL	(56)	(53)	(0.30)	(*R*)
				25	**96**	**0.24**	
3	0.5	2 × EtOAc/10 × heptane	(**2**)•spiro-TADDOL	(121)	(10)	(0.12)	(*R*)
				65	**31**	**0.20**	
4	1	4 × MeOH/16 × H_2O	(**2**)•spiro-TADDOL$_3$	(59)	(80)	(0.47)	(*R*)
				46	**98**	**0.45**	
5[h]	1	15 × H_2O	(**2**)•spiro-TADDOL$_2$	(79)	(88)	(0.69)	(*R*)
6[i]	1	15 × H_2O	(**2**)•spiro-TADDOL$_2$	(88)	(87)	(0.77)	(*R*)
				66	**98**	**0.65**	

[a] Mixture of solvents for the crystallization and recrystallizations [mL of solvent/g of resolving agent]. [b] The ratio of phosphine oxide (**2**) and the resolving agent was determined by ^{1}H NMR. [c] The yield of the diastereomer was calculated based on the half of the racemic phosphine oxide (**2**) that is regarded to be 100 % for each enantiomer. [d] Determined by HPLC using a chiral stationary phase. [e] Resolving capability, also known as the Fogassy parameter [*S* (–) = (Yield [%]/100) × (*ee* [%]/100)]. [f] The results obtained after the first crystallization are shown in parentheses, while the results obtained after purification(s) are shown in boldface. [g] Absolute configuration of the phosphine oxide (**2**) was determined by X-ray analysis (vide infra). [h] The temperature was 50 °C, and the crystallization time was 48 h. [i] The temperature was 50 °C, and the crystallization time was 168 h.

stereomer, indicating that the diastereomeric complex was unstable in that solvent mixture. This fact might be attributed to a competitive complexation of spiro-TADDOL [(*R*,*R*)-**9**] with alcohols, which was observed in our previous studies.[12e,26] Then, the resolution of racemic phosphine oxide **2** was also attempted in water. In order to avoid some issues caused by the low solubility, the resolution was accomplished at 50 °C, which gave us the best results after the first crystallization (*ee*: 88 %, yield: 79 %; Table 1, Entry 5). Such suspension-based resolution procedures can be found in the literature, but these results were somewhat unexpected, as either the racemic compound (**2**), or the resolving agent [(*R*,*R*)-**9**] is only partially soluble in water, and the reaction mixture was heterogeneous throughout the resolution process. However, we postulate that the hydrophilic media forcing the two lipophilic molecules together is responsible for the host–guest complexation, and consequently the enantiomeric recognition. With this promising preliminary result in hand, the reaction conditions, such as ratio of the racemic compound (**2**) and the spiro-TADDOL [(*R*,*R*)-**9**], ratio of the resolving agent [(*R*,*R*)-**9**] and water, temperature and time of the crystallization were optimized (See Supporting Information). It was found that crystallization at 50 °C for 168 h in the presence of 1 equivalent of spiro-TADDOL [(*R*,*R*)-**9**] (half-equivalent method) gave us the best results, and the diastereo-

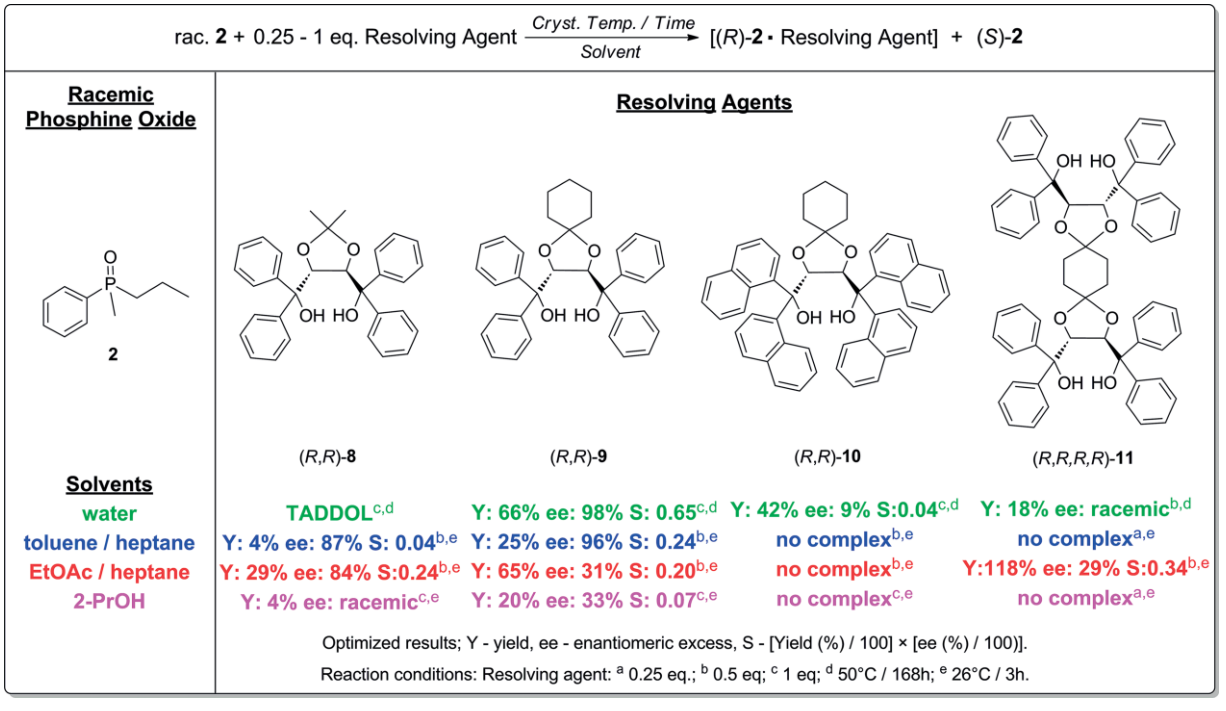

Figure 3. Comparison of the resolution of methyl-phenyl-propyl-phosphine oxide (**2**) with TADDOL-derivatives [(*R*,*R*)-**8**–(*R*,*R*,*R*,*R*)-**11**] (See Supporting Information Supplementary Table S4 for full details; "no complex" – no crystalline diastereomer was formed; "TADDOL" – the resolving agent precipitated, but no host–guest complex was formed).

meric complex could be purified by one recrystallization to give the (*R*)-methylphenylpropylphosphine oxide [(*R*)-**2**] with an *ee* of 98 % and in a yield of 66 %.

Having the suitable conditions in hand, we tested the applicability of other TADDOL-derivatives [(*R*,*R*)-**8**, (*R*,*R*)-**10** and (*R*,*R*,*R*,*R*)-**11**] for the enantiomeric separation of methylphenylpropylphosphine oxide (**2**). In our solvent and parameter optimization study, the best results (*ee* of 98 %) were obtained in water, and a high *ee* (96 %) could be obtained in a mixture of toluene and heptane (Table 1, Entries 2 and 6). Moreover, 2-propanol or a mixture of ethyl acetate and heptane led also to satisfactory results (Table 1, Entries 1 and 3).

Different resolving agents [(*R*,*R*)-**8**, (*R*,*R*)-**10** and (*R*,*R*,*R*,*R*)-**11**] were involved in this study to investigate whether the overall efficiency of the resolution can be improved by changing the structure of the resolving agent. Owing to the size-exclusion nature of OSN, the enlargement of the resolving agents [(*R*,*R*)-**10** and (*R*,*R*,*R*,*R*)-**11**] was explored to increase the molecular weight gap between the species to be separated, and to have more ideal separation with OSN (vide infra). The results are summarized in Figure 3, which also contains the results obtained with spiro-TADDOL [(*R*,*R*)-**9**].

Interestingly, the change in the structure of the resolving agent has an unexpectedly significant impact on the resolution efficiency. By changing the spiro-scaffold [(*R*,*R*)-**9**] to a dimethylketal [(*R*,*R*)-**8**] protecting group, the crystalline diastereomeric complexes could be obtained from toluene/heptane, EtOAc/heptane and 2-PrOH. However, the yields were low, and the maximum *ee* was 87 %. Changing the aromatic groups from phenyl to naphthyl had an even more pronounced effect, namely no diastereomers were formed with naphthyl-spiro-TADDOL [(*R*,*R*)-**10**] in most of the instances. Interestingly, water was the only solvent from which crystalline diastereomers were obtained, but the *ee* and efficiency remained low (*ee*: 9 %, *S*=0.04). The enantiomeric separation was also rather low with the bis-spiro-TADDOL [(*R*,*R*,*R*,*R*)-**11**], despite the fact that its structure shows a close resemblance to the structure of spiro-TADDOL [(*R*,*R*)-**9**]. The maximal *ee* was 29 % performing the crystallization of phosphine oxide (**2**) with bis-spiro-TADDOL [(*R*,*R*,*R*,*R*)-**11**] in a mixture of ethyl acetate and heptane. Using other solvents, either racemic phosphine oxide (**2**) was obtained, or no diastereomers were formed.

Resolution of Dialkyl-Arylphosphine Oxides (1–7) with spiro-TADDOL [(*R*,*R*)-9] Under Optimized Conditions

In our initial studies, the spiro-TADDOL [(*R*,*R*)-**9**] was selected as the most suitable resolving agent. The best results were obtained in water, in a mixture of toluene/heptane or ethyl acetate/heptane, and the conditions for crystallization were also established. In the next step, the substrate scope of this resolution procedure was investigated in the sphere of various dialkyl-arylphosphine oxides (**1–7**). The results are summarized in Figure 4.

The experiments indicated that the structure of the racemic compound (**1–7**) has also a significant impact on the overall efficiency of the optical resolution. Using water as the solvent, the (*R*)-enantiomer of the methyl-propyl-, ethyl-propyl- and the butyl-methyl- phenylphosphine oxides (**2–4**) was prepared with an *ee* of 95–98 %, and in a yield of 51–66 %. Interestingly, the efficiency of the resolution was significantly lower for these phosphine oxides (**2–4**), when the diastereomers were crystallized from toluene/heptane or ethyl acetate/heptane mixtures. This trend turned for the ethyl-methyl-, methyl-isopropyl- and the *c*-hexyl-methyl- phenylphosphine oxide (**1**, **5** and **6**) as the enantiomers or the enantiomeric mixture could be prepared only in the mixture of the organic solvents (*ee*: 31–99 %, yield: 21–56 %), whereas the application of water prevented the diastereomeric complex formation, or led to racemic phosphine oxide. Overall, the *tert*-butyl-methyl-phenylphosphine oxide (**7**)

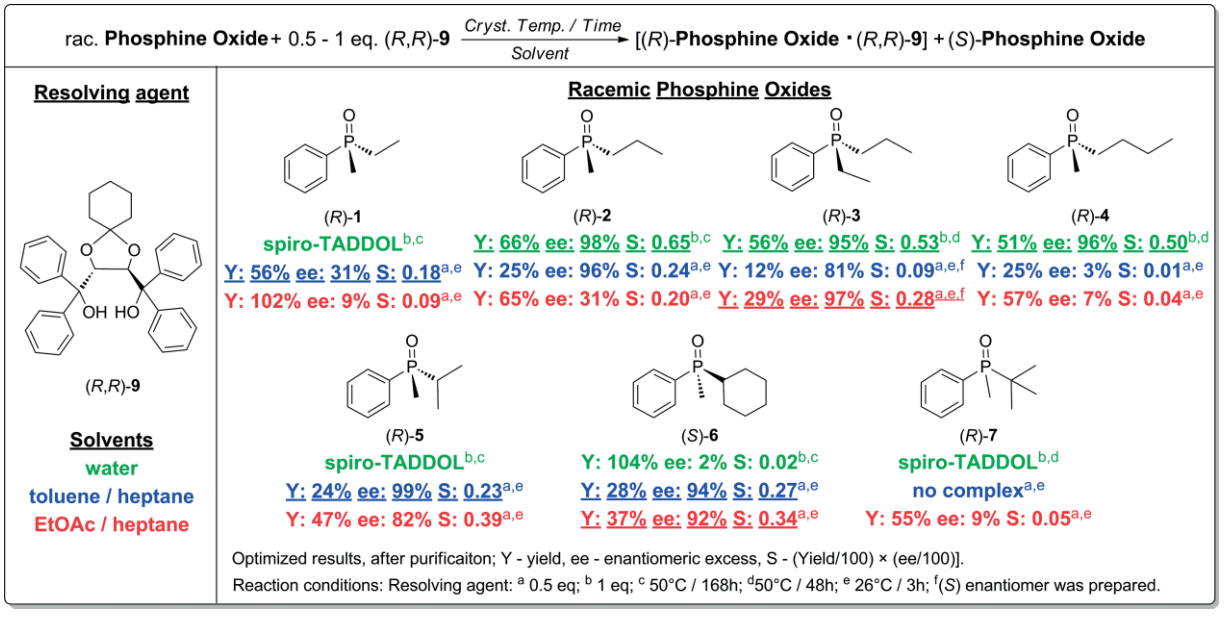

Figure 4. Comparison of the optical resolution of phosphine oxides (**1–7**) with spiro-TADDOL [(*R*,*R*)-**9**] under the optimized conditions.

was the only derivative, which could not be separated effectively into its enantiomers with spiro-TADDOL [(*R*,*R*)-**9**]. Moreover, the maximal enantiomeric purity reached for ethyl-methylphenylphosphine oxide [(*R*)-**1**] was only 31 %. These results might be attributed to steric factors, as the molecular size of the MeEtPhP(O) (**1**) might be too small for sufficient interaction between the host and the guest molecules, which is a prerequisite for a good enantiomeric recognition. Whereas, the increased steric bulk might be the reason for the inefficient resolution of *t*BuMePhP(O) (**7**).

On the other hand, the enantiomers of phosphine oxides **2**–**6** could be effectively separated by resolution with spiro-TADDOL [(*R*,*R*)-**9**] regardless of the size or the degree of branching of the alkyl chains, and the corresponding enantiomers were obtained with an *ee* of 94–99 % and in a yield of 21–65 %.

The optical resolutions with spiro-TADDOL [(*R*,*R*)-**9**] afforded the corresponding phosphine oxides enantiomers with (*R*) absolute configuration [(*R*)-**1**–(*R*)-**5**] in most of the instances regardless of the crystallization parameters. Interestingly, the (*S*) enantiomer could be prepared exclusively for *c*-hexyl-methylphenyl-phosphine oxide [(*S*)-**6**]. Moreover, the solvent had a great influence on the selection of the ethyl-phenylpropylphosphine (**3**) enantiomers incorporated into the diastereomeric complexes. The (*R*) enantiomer [(*R*)-**3**] could be prepared with spiro-TADDOL [(*R*,*R*)-**9**] in water, whereas enantiomeric mixtures containing the (*S*)-**3** enantiomer in excess could be prepared in toluene/heptane and ethyl acetate/heptane mixtures. The absolute configuration of the guest phosphine oxides (**1**–**7**) was determined by comparing the specific optical rotations with literature data. The absolute configuration of methylphenylpropylphosphine oxide and ethylphenylpropylphosphine oxide (**2** and **3**) was elucidated by X-ray crystallography (vide infra).

Complete Gram-Scale Optical Resolution Process for the Preparation of Both Enantiomers of Methylphenylpropylphosphine Oxide [(*R*)- and (*S*)-2] with (*R*,*R*)- and (*S*,*S*)-spiro-TADDOL [(*R*,*R*)- and (*S*,*S*)-9]

The optimization experiments were conducted on a millimolar scale, and as the next step, the resolution of methyl-phenyl-propyl-phosphine oxide (**2**) with (*R*,*R*)-spiro-TADDOL [(*R*,*R*)-**9**] was also accomplished on a gram scale. Besides demonstrating the scalability, the other aim of ours was to prepare both enantiomers of methylphenylpropylphosphine oxide [(*R*)- or (*S*)-**2**] (Scheme 4). The racemic methylphenylpropylphosphine oxide (**2**) was resolved with (*R*,*R*)-spiro-TADDOL [(*R*,*R*)-**9**] in water under the optimized conditions. After the purification and decomposition of the diastereomeric complex [(*R*)-**2**]•(spiro-TADDOL)$_2$, the (*R*)-enantiomer [(*R*)-**2**] was prepared with an *ee* of 98 % and in a yield of 72 %. To prepare the other enantiomer (*S*)-**2**, the mother liquors of the crystallization and recrystallization were combined, and the enantomeric mixture of (*S*)-**2** was separated from the traces of (*R*,*R*)-spiro-TADDOL [(*R*,*R*)-**9**]. The enantiomeric mixture of (*S*)-**2** (*ee*: 71 %) so obtained was resolved with (*S*,*S*)-spiro-TADDOL [(*S*,*S*)-**9**] in water, and the (*S*)-methylphenylpropylphosphine oxide [(*S*)-**2**] could be obtained with an *ee* of 98 % and in a yield of 45 % after one crystallization followed by the decomposition of the corresponding diastereomer. These results indicate that the optimized resolution

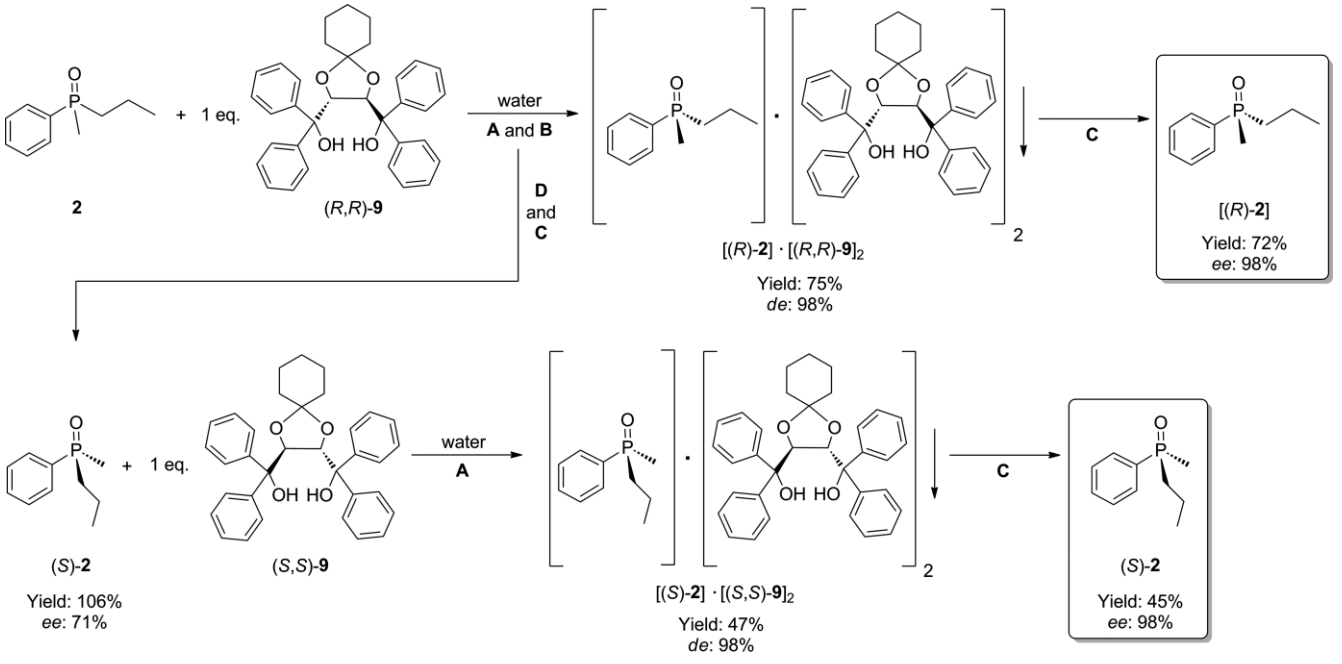

A: crystallization (50°C - 168 h); **B**: recrystallization (50°C - 168 h); **C**: column chromatography; **D**: extraction

[a] The yield was calculated based on the half of the racemic phosphine oxide (**2**) that is regarded to be 100% for each antipode.

Scheme 4. Gram-scale preparation of both enantiomers of methylphenylpropylphosphine oxide [(*R*)- or (*S*)-**2**] on with (*R*,*R*)- and (*S*,*S*)-spiro-TADDOL [(*R*,*R*)-**9** and (*S*,*S*)-**9**].

procedures for phosphine oxides **1**–**6** can be accomplished on gram scale with similar efficiency. Moreover, the other enantiomer of the target phosphine oxide (**1–6**) can be obtained from the mother liquor using the (*S*,*S*) enantiomer of spiro-TADDOL [(*S*,*S*)-**9**] under similar crystallization conditions.

Single Crystal and Powder X-ray Analysis of a Few Diastereomeric Complexes

Crystallinity of the diastereomers prepared from the corresponding phosphine oxide (**1–7**) and spiro-TADDOL [(*R*,*R*)-**9**] was checked by powder X-ray diffraction. Additionally, single crystals were successfully grown from the diastereomers containing spiro-TADDOL [(*R*,*R*)-**9**] and (*R*)-methylphenylpropylphosphine oxide [(*R*)-**2**] or (*S*)-ethyl-phenylpropylphosphine oxide [(*S*)-**3**] allowing us to investigate the second order interactions responsible for the enantiomeric recognition. Moreover, the direct comparison of the two crystals gave some insight how the crystal structures and the interactions may alter when phosphine oxides [(*R*)-**2** and (*S*)-**3**] with different structure and absolute configuration are present.

The single-crystal X-ray analysis confirmed that the diastereomers contained the spiro-TADDOL [(*R*,*R*)-**9**] and the corresponding phosphine oxide [(*R*)-**2** or (*S*)-**3**] enantiomer in a 1:1 ratio, which was in accordance with the NMR studies. ORTEP style molecular structure diagram can be found in Figure 5. Similar unit cell parameters were measured for the two selected crystals indicating similarities of the (*R*,*R*)-spiro-TADDOL [(*R*,*R*)-**9**], the (*R*)-**2** or (*S*)-**3** guest molecules and hydrogen bond systems within. The Cell Similarity Index is (Π_l) 0.10901.

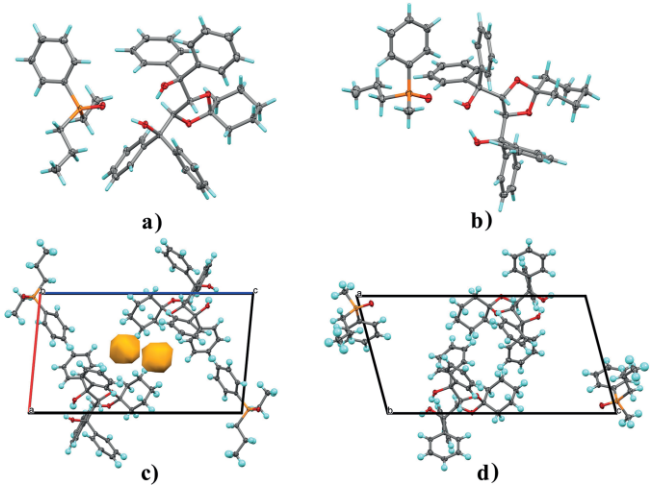

Figure 5. The crystallographically independent molecules in the asymmetric unit of the crystal a.) [(*S*)-**3**]•spiro-TADDOL and b.) [(*R*)-**2**]•spiro-TADDOL without the atomic labelling. Displacement ellipsoids are drawn at the 30 % probability level for clarity. The observable voids in the crystal lattices c.) [(*S*)-**3**]•spiro-TADDOL and d.) [(*R*)-**2**]•spiro-TADDOL. Two small voids in the crystal lattice are displayed in orange colour in the case of [(*S*)-**3**]•spiro-TADDOL.

The density is 1.244 for the [(*R*)-**2**]•spiro-TADDOL and 1.210 for the [(*S*)-**3**]•spiro-TADDOL diastereomer. The Kitaigorodsky Packing Index (K.P.I)[27] values were also similar {67.9 % and 66.4 % for the [(*R*)-**2**]•spiro-TADDOL and [(*S*)-**3**]•spiro-TADDOL, respectively}. However, despite these similar density and K.P.I. values, the two crystals are not isostructural, as the guest phosphine oxides [(*R*)-**2** or (*S*)-**3**] have different places in the unit cell. Moreover, two small voids were found in the crystal structure of the [(*S*)-**3**]•spiro-TADDOL complex, which were not present in the crystal structure of the [(*R*)-**2**]•spiro-TADDOL diastereomer (Figure 5.). These voids have a volume of ca. 2 × 33 Å^3, which size is not enough for the incorporation of smaller solvent molecules (e.g. water needed 40 Å^3).

Intriguingly, the absolute configuration of the phosphine oxide guest molecules [(*R*)-**2** or (*S*)-**3**] is the opposite, despite the structural similarity and the same configuration of the host spiro-TADDOL [(*R*,*R*)-**9**] molecule.

The interactions between the (*R*)-**2** or (*S*)-**3** phosphine oxides and the spiro-TADDOL [(*R*,*R*)-**9**] were investigated with Hirshfeld surface by the Crystal Explorer program (See Supporting Information for details). The Hishfeld surface fingerprints indicated that the short and strong intermolecular interactions (i.e. hydrogen bonds) are similar, and the main differences could be found in the weaker interactions. More longer and weaker contacts can be found in the crystal structure of the [(*S*)-**3**]•spiro-TADDOL diastereomer than in the crystal lattice of [(*R*)-**2**]•spiro-TADDOL. Moreover, the atom-type Hirshfeld interpretations also showed significant dissimilarities within the weak intermolecular interactions between specific atomic types. The Hirshfeld fingerprint interpretation shows the difference in atomic position and distances, but it is unable to characterize the energies associated with these contacts. Thus, some DFT calculations were made by the Crystal Explorer12 program on the B3LYP/6-31G(d,p) level of theory for better understanding the interactions between the host and guest molecules.

The crystal structures and the DFT calculations revealed several contacts. The most relevant atomic distances, as well as the results of the calculations are summarized in Figure 6. The two OH groups of the spiro-TADDOL [(*R*,*R*)-**9**] form an intramolecular *H*-bond, which is characteristic to the TADDOL-type molecules.[12f] Thus, one hydroxyl group of (*R*,*R*)-**9** is capable of the formation of an intermolecular *H*-bridge with the corresponding phosphine oxide enantiomer [(*R*)-**2** or (*S*)-**3**]. The atomic distances indicate (2.686 Å and 2.634 Å) that this *H*-bridge is the strongest intermolecular contact. CH•••π interactions can also be observed, but there are differences in the two crystal lattices. In case of the (*S*)-ethyl-phenylpropylphosphine oxide [(*S*)-**3**], a CH_2•••π interaction is present, whereas a T-spape π•••π contact can be observed between the aryl groups of the methylphenylpropylphosphine oxide [(*R*)-**2**] and the spiro-TADDOL [(*R*,*R*)-**9**]. The interactions formed between the two phosphine oxide molecules are also different. There is a CH••• π contact between the two MePrPhP(O) molecules [(*R*)-**2**], whereas a CH•••O=P contact can be found between the two (*S*)-ethyl-phenylpropylphosphine oxides [(*S*)-**3**].

The DFT results also confirmed that the strongest force is a coulomb interaction between the hydrogen bridge acceptor phosphine oxides [(*R*)-**2** or (*S*)-**3**] and the hydrogen-bond donor (*R*,*R*)-spiro-TADDOL [(*R*,*R*)-**9**] in both crystal structures. The second strongest interaction is within two neighbouring phosphine oxide moieties [(*R*)-**2** or (*S*)-**3**] caused by the polarization

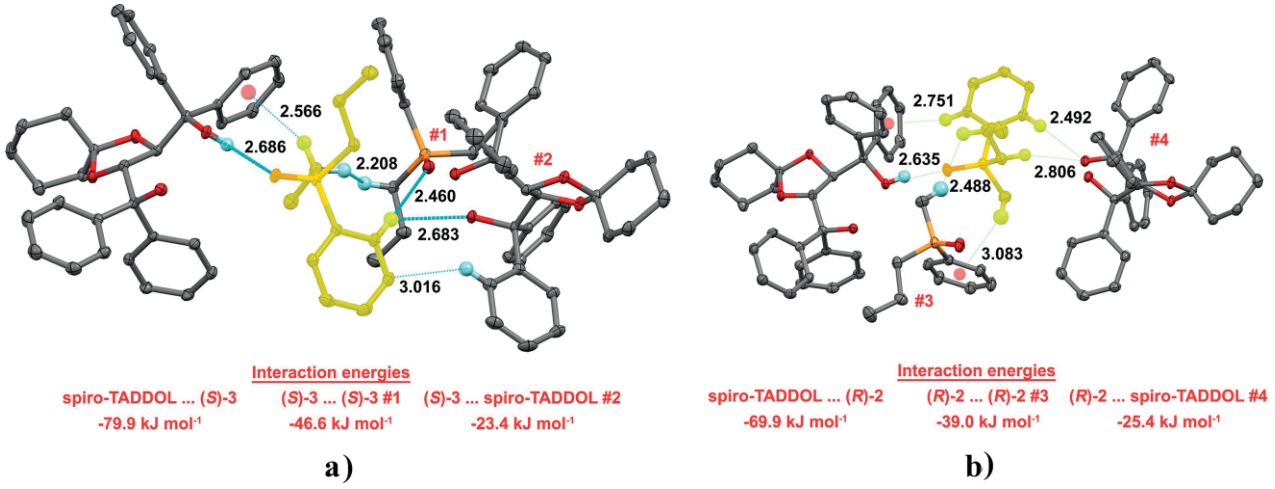

Figure 6. A few representative atomic distances and the strongest total energies among the neighbouring molecules for the [(*S*)-**3**]•spiro-TADDOL (**a**) and [(*R*)-**2**]•spiro-TADDOL (**b**). The yellow highlight represents the selected phosphine oxide [(*R*)-**2** or (*S*)-**3**] for the calculation of interaction energies.

of the P=O moiety. The third strongest interaction is observed between the other spiro-TADDOL molecule and the corresponding methylpropyl- and ethylpropyl-phenyl-phosphine oxide [(*R*)-**2** or (*S*)-**3**]. These weak London dispersion forces are caused by the high overlapping surfaces of the (*R*)-**2** or (*S*)-**3** guest and the (*R*,*R*)-**9** host molecule. However, the calculations revealed that the energetics of these interactions are rather different in the two crystal lattices (Figure 6.). Thus, despite the structural similarities of the two phosphine oxides [(*R*)-**2** or (*S*)-**3**], significant differences were found both in the nature and the strength of these second order interactions, which may be an underlying reason for the different enantiopreference in case in the two crystal structures.

We were unable to grow X-ray quality crystals from the diastereomers prepared in aqueous media. Thus, these crystalline samples were subjected to powder X-ray measurements along with a few crystals prepared in organic solvents in order to seek for structural similarities between the diastereomeric molecular complexes. First, the [(*R*)-**2**]•spiro-TADDOL diastereomer was investigated, and the powder XRD-pattern measured at room temperature has been compared with that of generated from the atomic coordinates obtained by the single crystal structural determination at temperature of 148 K (Figure 7a and Figure 7b). The series of diffraction peak positions are in good agreement considering the experimental profile and the corresponding simulated pattern, which indicates that the measured single crystal was representative for the solid state obtained by optical resolution. Slight differences are arising from the temperature difference of XRD-measurements resulting in extension or contraction of the crystal lattice as a whole, and its interplanar lattice distances, as well. There is a considerable alteration in the relative intensity of diffraction peaks, probably because of a kind of preferred orientation of sample crystal set at the measurement of powder profile. Despite the latter observation, an indexing of the room temperature powder pattern shows very similar, but increased unit cell parameters to those obtained by the single crystal measurement (See Supporting Information, Supplementary Table S13 for details).

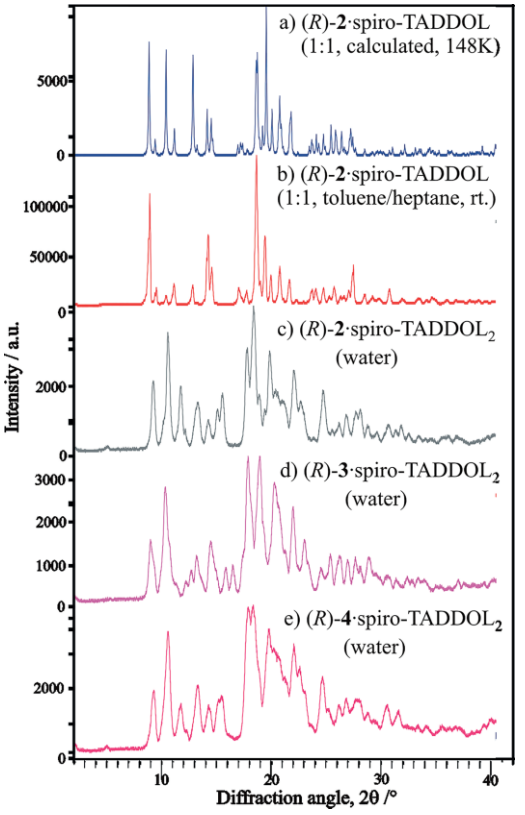

Figure 7. Comparison of powder XRD profiles of a few selected diastereomeric complexes.

Figure 7 c also shows that the [(*R*)-**2**]•spiro-TADDOL$_2$ diastereomer prepared from aqueous media exhibited a powder XRD profile quite different from that prepared from a mixture of toluene and heptane (Figure 7a and Figure 7b). There are significant differences in the positions of the diffraction peaks referring to different dominating crystalline structures. The reason for the different powder XRD profiles is the different stoichiometric molar ratio of the (*R*)-methylphenylpropyl-

phosphine oxide [(*R*)-**2**] and the (*R*,*R*)-spiro-TADDOL [(*R*,*R*)-**9**], which also results in different orientations and interactions among the host and the guest molecules. The enantiopure (*R*)-ethylpropyl- or the (*R*)-butylmethyl-phenylphosphine oxides [(*R*)-**3** or (*R*)-**4**] could also be prepared with (*R*,*R*)-spiro-TADDOL [(*R*,*R*)-**9**] in water. Thus, the host–guest complexes of [(*R*)-**3**]•spiro-TADDOL$_2$ or [(*R*)-**4**]•spiro-TADDOL$_2$ were also subjected to powder XRD analysis. Surprisingly, the X-ray diffraction profiles of the [(*R*)-**2**]•spiro-TADDOL$_2$ and [(*R*)-**4**]•spiro-TADDOL$_2$ diastereomers prepared in aqueous media showed similar pattern (Figure 7c and Figure 7e). Despite the different guest molecules [(*R*)-**2** or (*R*)-**4**], these two diastereomeric co-crystals may be considered isomorphic, or at least isostructural ones, indicating similar mode and spatial arrangements of binding and interactions between the given phosphine oxides [(*R*)-**2** or (*R*)-**4**] and the (*R*,*R*)-spiro-TADDOL [(*R*,*R*)-**9**]. Interestingly, these two diffraction profiles were different from that of [(*R*)-**3**]•spiro-TADDOL$_2$ (Figure 7d), indicating that changing a methyl group to ethyl group may significantly alter the interactions within the diastereomeric complex resulting in a different crystal structure. It is noteworthy, that an increased peak broadening also occurred in all the samples of aqueous origin, probably because of their lowered crystallinity or microcrystalline feature.

Comparison of the Column Chromatographic and Nanofiltration-Enabled Decomposition of Diastereomeric Complexes and Recovery of Phosphine Oxide (1–7) Enantiomers and Resolving Agents [(*R*,*R*)-9–(*R*,*R*,*R*,*R*)-11]

As the volatility of the phosphine oxides (**1–7**) is low, column chromatography is used for the decomposition of the corresponding diastereomeric complexes and for the recovery of the (*R*)-methylphenylpropylphosphine oxide [(*R*)-**2**] and (*R*,*R*)-spiro-TADDOL [(*R*,*R*)-**9**]. Several solvents were tested for the chromatographic separation (See Supporting Information for the complete list). Our goal was to find a solvent or solvent system, which allows complete separation of the two compounds [(*R*)-**2** and (*R*,*R*)-**9**] without obtaining mixed fractions. The DCM to DCM/MeOH mixture was our choice in our previous studies,[12e,12f] and this solvent system seemed suitable based on the TLC analysis. However, we intended to choose other solvents, which met more criteria of green chemistry and suitability for industrial use.[28] Thus, we chose a EtOAc to EtOAc/2-PrOH gradient elution based on our TLC tests.

For comparison, the same sample was separated under same flash chromatographic conditions (stationary phase; flow rate; fraction volume etc.). To our delight both solvent systems (DCM to DCM/MeOH or EtOAc to EtOAc/2-PrOH) were appropriate for separation with flash chromatography. The advantages of these solvents is that the resolving agent [(*R*,*R*)-**9**] could be removed completely under isocratic conditions using pure DCM or EtOAc.

Then, the (*R*)-**2** phosphine oxide enantiomer could be eluted from the column applying a DCM/MeOH or EtOAc/2-PrOH gradient. In this manner no mixed fractions containing both (*R*)-**2** and (*R*,*R*)-**9** were obtained. The recovery of (*R*)-methyl-phenyl-propyl-phosphine oxide [(*R*)-**2**] and (*R*,*R*)-spiro-TADDOL [(*R*,*R*)-**9**] was above 96 % in all cases (Figure 8.). Considering the two column chromatographic methods, 370 or 310 mL of solvent was used for the decomposition of 600 mg of diastereomers, as well as for the recovery of ca. 500 mg of the resolving agent [(*R*,*R*)-**9**] and 100 mg of the (*R*)-methylphenylpropylphosphine oxide [(*R*)-**2**]. As 6 empty fractions were collected in both cases, one may argue that the solvent consumption can be lowered by ca. 50 mL using a more optimized gradient.

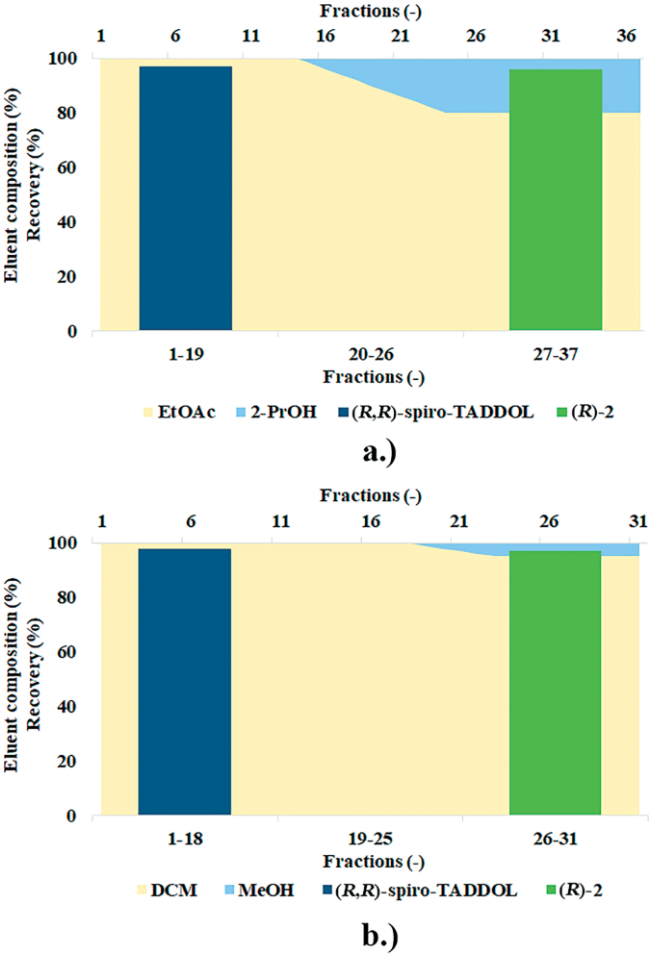

Figure 8. Evaluation of the recovery of (*R*)-methylphenylpropylphosphine oxide [(*R*)-**2**] and (*R*,*R*)-spiro-TADDOL [(*R*,*R*)-**9**] from the corresponding diastereomer by flash chromatography [The bars show the recovery of (*R*)-**2** and (*R*,*R*)-**9**, while the area-chart show the change in eluent composition].

Organic solvent nanofiltration could serve as a scalable technique for the decomposition of the diastereomeric complexes, and the recovery of the phosphine oxide enantiomers. First, the use of organic solvent nanofiltration was explored using NP030P membrane by Nadir and methanol as the solvent. The molecular weight cut-off (MWCO) curve of the membrane was determined for the dialkyl-arylphosphine oxides (**1–7**), and the resolving agents incorporating the spiro-TADDOL scaffold [(*R*,*R*)-**9**–(*R*,*R*,*R*,*R*)-**11**] (Figure 9). In order to maximize the rejection of the resolving agents [(*R*,*R*)-**9**–(*R*,*R*,*R*,*R*)-**11**], the membrane was treated with branched polyethylene glycol (PEG) having 2,600 g mol^{-1} molecular weight.

The PEG treatment resulted in tighter membranes with increased rejections (Figure 9). This change was beneficial for the

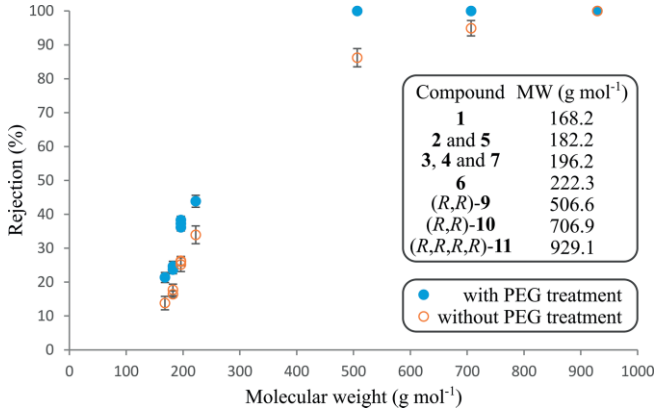

Figure 9. Molecular weight cut-off (MWCO) curve for Nadir NP030P membrane with and without treatment with branched PEG in methanol at 40 bar pressure.

resolving agents [(*R*,*R*)-**9**–(*R*,*R*,*R*,*R*)-**11**], which are to be retained by the membrane during diafiltration. The most prominent increase in rejection from 86.2 ± 2.7 % to 100 % was obtained for the best resolving agent, spiro-TADDOL [(*R*,*R*)-**9**]. Figure 9. also shows that the rejection values for the dialkyl-arylphoshine oxides (**1–7**) were in the range of 13.8 ± 2.0 % – 34.0 ± 2.6 % with the original Nadir NP030P membrane, and these values slightly increased to 21.4 ± 1.5 % – 43.9 ± 1.8 % after the PEG treatment. The low rejection values of the phosphine oxide (**1–7**) compared to complete rejection of the resolving agents [(*R*,*R*)-**9**–(*R*,*R*,*R*,*R*)-**11**] were sufficient for a nanofiltration-based separation strategy.

Based on the rejection results, the [(*R*)-**2**]•(spiro-TADDOL)$_2$ molecular complex was selected for the decomposition of the diastereomer, as well as for the recovery of (*R*)-methylphenylpropylphosphine oxide [(*R*)-**2**] and (*R*,*R*)-spiro-TADDOL [(*R*,*R*)-**9**] using the PEG-treated NP030P membrane. The simulated diafiltration separation (lines) and the experimental data (symbols) for processing the diastereomeric complex [(*R*)-**2**]•(spiro-TADDOL)$_2$ are shown in Figure 10. The (*R*)-**2** phosphine oxide was purged out of the system and virtually 100 % purity of the spiro-TADDOL [(*R*,*R*)-**9**] was achieved within less than 8 diavolumes (Figure 10a). In this experiment, ca. 1.3 g of (*R*)-**2**•(spiro-TADDOL)$_2$ diastereomeric complex was decomposed. As nearly complete separation of (*R*)-**2** phosphine oxide and spiro-TADDOL [(*R*,*R*)-**9**] was achieved in 6–7 diavolumes, the solvent consumption was in the range of 470–550 mL of solvent per gram of diastereomer. The robustness of the purification methodology was investigated through varying the theoretical rejection of (*R*,*R*)-**9** from 99.5 % to 100 % (Figure 10b). As the rejection decreases, the purity of (*R*)-methylphenylpropylphosphine oxide [(*R*)-**2**] significantly decreases due to the fact that the concentration of spiro-TADDOL [(*R*,*R*)-**9**] in the feed stream is considerably higher. Even a small leakage of the resolving agent through the membrane (i.e. incomplete rejection) results in a significant contamination of (*R*)-**2** in the permeate stream. On the contrary, the increase in the loss of (*R*,*R*)-**9** as a function of its rejection (100 % → 99.5 %) is less pronounced (0 % → 5 %). These results show the importance of obtaining complete rejection of the resolving agents, which is easier to achieve by having large molecular weights.

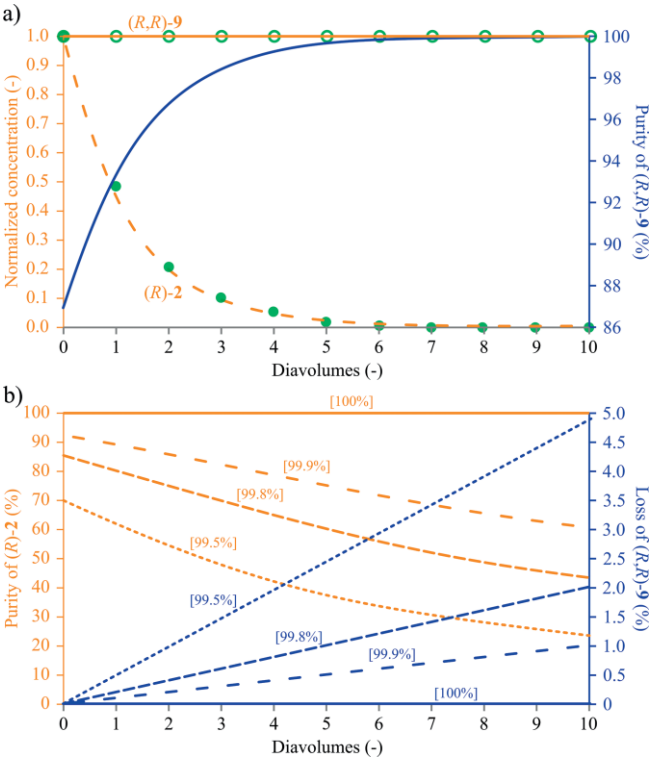

Figure 10. Concentration profiles during the diafiltration of the [(*R*)-**2**]•(spiro-TADDOL)$_2$ diastereomer and the purity of the resolving agent in the retentate stream (a); and the effect of (*R*,*R*)-**9** rejection (see values in brackets) on the purity of (*R*)-**2** in the permeate stream caused by the loss of (*R*,*R*)-**9** from the retentate (b).

Conclusion

In this paper, the resolution of a series of phosphine oxides was investigated with TADDOL-derivatives [(*R*,*R*)-**8**–(*R*,*R*,*R*,*R*)-**11**]. It was demonstrated, that this resolving agent class, especially the spiro-TADDOL [(*R*,*R*)-**9**] is applicable for the enantioseparation of these challenging substrates, which have limited capabilities to form second order interactions due to the presence of two alkyl groups. The results showed that there is an ideal molecular size for the sufficient enantioseparation. The MeEtPhP(O) (**1**) have small molecular size, whereas the increased steric bulk might be the reason for the inefficient resolution of *t*BuMePhP(O) (**7**). The enantiomers of other five dialkyl-arylphosphine oxides (**2–6**) were prepared with enantiomeric excess values greater than 94 %. During the optimization of the crystallization conditions, two separate crystallization methods were developed, one utilized organic solvent and the other one used water. This is one of the handful successful examples for performing enantioseparations with TADDOL-derivatives in aqueous media. A gram-scale resolution was performed demonstrating the scalability of this method, and both enantiomers of the methylphenylpropylphosphine oxide (**2**) were prepared with (*R*,*R*)- or (*S*,*S*)-spiro-TADDOL [(*R*,*R*)- or (*S*,*S*)-**9**]. The structure of a few diastereomeric complexes were investigated by single crystal or powder X-ray crystallography, and the main secondary interactions responsible for the enantiomeric recognition were also identified. Nadir NP030P membrane was successfully employed in a diafiltration process for the gram-scale separa-

tion of the enantiopure (*R*)-methylphenylpropylphosphine oxide [(*R*)-**2**], and the TADDOL-based resolving agent [(*R*,*R*)-**9**]. The use of a branched PEG for the preconditioning of the membrane was found to be a useful tool to tighten the membrane and increase solute rejection. The presented OSN methodology could be further exploited for the recovery of other resolving agents, and the parallel isolation of enantiopure products.

Experimental Section

Materials and Apparatus: The details of the chemicals, the instruments used in this study, as well as the synthetic procedures for the preparation of phosphine oxides (**1–7**) and resolving agents [(*R*,*R*)-**8**–(*R*,*R*,*R*,*R*)-**11**] can be found in the Supporting Information.

Representative Resolution Procedures

Resolution of Methylphenylpropylphosphine Oxide (2) with spiro-TADDOL [(*R*,*R*)-9] Using the Crystallization Method (Method I): 0.10 g (0.55 mmol) of Racemic methylphenylpropylphosphie oxide (**2**) and 0.28 g (0.55 mmol) of spiro-TADDOL [(*R*,*R*)-**9**] were dissolved in 1.7 mL of hot isopropyl-alcohol. Colorless crystalline diastereomeric complex of (*R*)-**2**•(spiro-TADDOL)$_2$ appeared after cooling the mixture to 25 °C. After standing at 25 °C for 3 hours, the crystals were separated by filtration to give 0.21 g (64 %) of (*R*)-**2**•(spiro-TADDOL)$_2$ with a *de* of 35 %. The diastereomeric complex (*R*)-**2**•(spiro-TADDOL)$_2$ was purified by recrystallization according to the procedure described above from 1.7 mL of isopropyl-alcohol to afford 0.066 g (20 %) of the (*R*)-**2**•(spiro-TADDOL)$_2$ with a *de* of 33 % (Table 1, Entry 1). The (*R*)-methylphenylpropylphosphine oxide [(*R*)-**2**] was recovered from the diastereomer by flash column chromatography (silica gel, gradient elution, ethyl acetate to ethyl acetate/isopropyl-alcohol, 80:20) to give 0.009 g (18 %) of (*R*)-methylphenylpropylphosphine oxide [(*R*)-**2**] with an *ee* of 33 %.

Resolution of Methylphenylpropylphosphine Oxide (2) with spiro-TADDOL [(*R*,*R*)-9] Using the Precipitation Method (Method II): 0.051 g (0.28 mmol) of Racemic methylphenylpropylphosphine oxide (**2**) and 0.071 g (0.14 mmol) of spiro-TADDOL [(*R*,*R*)-**9**] were dissolved in 0.35 mL of hot toluene, and then 0.35 mL of heptane was added. Colorless crystalline diastereomeric complex of (*R*)-**2**•(spiro-TADDOL) appeared immediately. After standing at 25 °C for 3 hours, the crystals were separated by filtration to give 0.054 g (56 %) of (*R*)-**2**•(spiro-TADDOL) with a *de* of 53 %. The diastereomeric complex (*R*)-**2**•(spiro-TADDOL) was purified by two recrystallizations according to the procedure described above from a mixture of 0.35 mL of toluene and 0.35 mL of heptane to afford 0.024 g (25 %) of the (*R*)-**2**•(spiro-TADDOL) with a *de* of 96 % (Table 1, Entry 2). The (*R*)-methylphenylpropylphosphine oxide [(*R*)-**2**] was recovered from the diastereomer by flash column chromatography (silica gel, gradient elution, ethyl acetate to ethyl acetate/isopropyl-alcohol, 80:20) to give 0.0057 g (22 %) of (*R*)-methylphenylpropylphosphine oxide [(*R*)-**2**] with an *ee* of 96 %.

Resolution of Methylphenylpropylphosphine Oxide (2) with spiro-TADDOL [(*R*,*R*)-9] Using the Suspension Method (Method III.): A suspension of 0.052 g (0.28 mmol) of racemic methylphenylpropylphosphine oxide (**2**) and 0.14 g (0.28 mmol) spiro-TADDOL [(*R*,*R*)-**9**] was stirred in 2.2 mL of water at 50 °C for 1 week. The crystals were then separated by filtration to give 0.15 g (88 %) of (*R*)-**2**•(spiro-TADDOL)$_2$ with a *de* of 87 %. The diastereomeric complex (*R*)-**2**•(spiro-TADDOL)$_2$ was purified by stirring the crystals in 2.2 mL of water at 50 °C for 1 week to afford 0.11 g (66 %) of (*R*)-**2**•(spiro-TADDOL)$_2$ with a *de* of 98 % (Table 1, Entry 6). The (*R*)-methylphenylpropylphosphine oxide [(*R*)-**2**] was recovered from the diastereomer by flash column chromatography (silica gel, gradient elution, ethyl acetate to ethyl acetate/isopropyl-alcohol, 80:20) to give 0.015 g (60 %) of (*R*)-methylphenylpropylphosphine oxide [(*R*)-**2**] with an *ee* of 98 %.

Separation of the Phosphine Oxides (1–7) and the Resolving Agents [(*R*,*R*)-9–(*R*,*R*,*R*,*R*)-11] Organic Solvent Nanofiltration: The feed solution for the molecular weight cut-off (MWCO) determination comprised a single-solute phosphine oxide (**1–7**) or resolving agent [(*R*,*R*)-**9**–(*R*,*R*,*R*,*R*)-**11**] at 0.1 g L^{-1} concentration in methanol at 40 bar. The Nadir NP030P membrane with an area (A) of 52.8 cm^2 was used with and without treatment with a 1 g L^{-1} branched PEG having a molecular weight of 2,600 g mol^{-1} for 24 h. The membrane were conditioned in methanol at 40 bar for 24 hours in a cross-flow nanofiltration rig (Supplementary Figure 1.) as described earlier.[21] A recirculation gear pump was set at 1 L min^{-1} to ensured homogeneous solute concentration and mitigate concentration polarization in the retentate loop. The mathematical framework for the diafiltration modeling of the concentration profiles and purities were previously reported.[29] The solute rejections (*R*) were determined as the ratio of the permeate (C_p) and retentate (C_r) concentrations [Equation (1)]:

$$R\ [\%] = (1 - \frac{C_p}{C_f}) \times 100 \quad (1)$$

The reported results are averages of two independently performed experiments. The permeance (*P*) was determined as the volume of permeate divided by the applied pressure (ΔP), membrane area (*A*) and time (*t*) [Equation (2)]:

$$P\ [\mathrm{Lm^{-2}h^{-1}\ bar^{-1}}] = \frac{V}{\Delta P \cdot A \cdot t} \quad (2)$$

During the diafiltration 1.27 g of diastereomer complex (*R*)-**2**•(spiro-TADDOL)$_2$ was loaded onto the membrane in 100 mL of methanol. The filtration was performed at 40 bar, and fresh solvent was continuously added in order to compensate the permeate volume leaving the system, keeping the system volume constant at 100 mL. The filtration was performed up to 10 diavolumes [*D*, Equation (3)], which is defined as the ratio of added solvent volume (V_{add}) and system volume (V_{system}):

$$D = \frac{V_{add}}{V_{system}} \quad (3)$$

X-ray Measurements: Summary of crystallographic data, data collections, structure determination and refinement for [(*R*)-**2**]•spiro-TADDOL and [(*S*)-**3**]•spiro-TADDOL is listed in Supplementary Table S9.

CCDC 1957408 {for [(*R*)-**2**]•spiro-TADDOL}, and 1957409 {for [(*S*)-**3**]•spiro-TADDOL} contain the supplementary crystallographic data for this paper. These data can be obtained free of charge from The Cambridge Crystallographic Data Centre.

Acknowledgments

This work was supported by the National Research, Development and Innovation Office - NKFIH (Grant No. OTKA PD 116096). Tamás Holczbauer is grateful for the support of the National Research, Development and Innovation Office-NKFIH (Grant No. OTKA PD 128504) and the János Bolyai Research Scholarship of the HAS. György Székely acknowledges the financial support from KAUST.

Keywords: Chiral resolution · Acyclic phosphine oxides · Supramolecular investigation · Organic solvent nanofiltration

[1] a) A. Grabulosa, *P-Stereogenic Ligands in Enantioselective Catalysis*, The Royal Society Of Chemistry, Cambridge, **2010**; b) M. Dutartre, J. Bayardon, S. Jugé, *Chem. Soc. Rev.* **2016**, *45*, 5771–5794.

[2] a) P. C. J. Kamer, P. W. N. M. Van Leeuwen, Phosphorus(III)Ligands in Homogeneous Catalysis: Design and Synthesis, John Wiley & Sons, New York, **2012**; b) W. Fu, W. Tang, *ACS Catal.* **2016**, *6*, 4814–4858; c) T. Imamoto, *Chem. Rec.* **2016**, *16*, 2659–2669.

[3] a) Y. Xiao, Z. Sun, H. Guo, O. Kwon, *Beilstein J. Org. Chem.* **2014**, *10*, 2089–2121; b) H. Guo, Y. C. Fan, Z. Sun, Y. Wu, O. Kwon, *Chem. Rev.* **2018**, *118*, 10049–10293; c) H. Ni, W.-L. Chan, Y. Lu, *Chem. Rev.* **2018**, *118*, 9344–9411; d) M. Benaglia, S. Rossi, *Org. Biomol. Chem.* **2010**, *8*, 3824–3830; e) S. Kotani, *Chem. Pharm. Bull.* **2019**, *67*, 519–526; f) T. Ayad, A. Gernet, J.-L. Pirat, D. Virieux, *Tetrahedron* **2019**, *75*, 4385–4418; g) S. Liu, Y. Kumatabara, S. Shirakawa, *Green Chem.* **2016**, *18*, 331–341; h) A. Golandaj, A. Ahmad, D. Ramjugernath, *Adv. Synth. Catal.* **2017**, *359*, 3676–3706.

[4] J. Chrzanowski, D. Krasowska, J. Drabowicz, *Heteroat. Chem.* **2018**, *29*, e21476.

[5] D. Herault, D. H. Nguyen, D. Nuel, G. Buono, *Chem. Soc. Rev.* **2015**, *44*, 2508–2528.

[6] a) R. Beaud, R. J. Phipps, M. J. Gaunt, *J. Am. Chem. Soc.* **2016**, *138*, 13183–13186; b) Y. S. Jang, Ł. Woźniak, J. Pedroni, N. Cramer, *Angew. Chem. Int. Ed.* **2018**, *57*, 12901–12905; *Angew. Chem.* **2018**, *130*, 13083; c) X.-T. Liu, Y.-Q. Zhang, X.-Y. Han, S.-P. Sun, Q.-W. Zhang, *J. Am. Chem. Soc.* **2019**, *141*, 16584–16589.

[7] a) F. Chaux, S. Frynas, H. Laureano, C. Salomon, G. Morata, M.-L. Auclair, M. (Massoud) Stephan, R. Merdès, P. Richard, M.-J. Ondel-Eymin, et al., *C. R. Chim.* **2010**, *13*, 1213–1226; b) Z. S. Han, N. Goyal, M. A. Herbage, J. D. Sieber, B. Qu, Y. Xu, Z. Li, J. T. Reeves, J.-N. Desrosiers, S. Ma, et al., *J. Am. Chem. Soc.* **2013**, *135*, 2474–2477; c) L. Copey, L. Jean-Gérard, E. Framery, G. Pilet, V. Robert, B. Andrioletti, *Chem. Eur. J.* **2015**, *21*, 9057–9061; d) A. D'Onofrio, L. Copey, L. Jean-Gérard, C. Goux-Henry, G. Pilet, B. Andrioletti, E. Framery, *Org. Biomol. Chem.* **2015**, *13*, 9029–9034; e) S.-G. Li, M. Yuan, F. Topic, Z. S. Han, C. H. Senanayake, Y. S. Tsantrizos, *J. Org. Chem.* **2019**, *84*, 7291–7302.

[8] a) O. Korpiun, R. A. Lewis, J. Chickos, K. Mislow, *J. Am. Chem. Soc.* **1968**, *90*, 4842–4846; b) U. Schmidt, B. Riedl, H. Griesser, C. Fitz, *Synthesis* **1991**, 655–657; c) N. G. Andersen, P. D. Ramsden, D. Che, M. Parvez, B. A. Keay, *Org. Lett.* **1999**, *1*, 2009–2011; d) N. G. Andersen, P. D. Ramsden, D. Q. Che, M. Parvez, B. A. Keay, *J. Org. Chem.* **2001**, *66*, 7478–7486; e) M. Oliana, F. King, P. N. Horton, M. B. Hursthouse, K. K. (Mimi) Hii, *J. Org. Chem.* **2006**, *71*, 2472–2479; f) H. Adams, R. C. Collins, S. Jones, C. J. A. Warner, *Org. Lett.* **2011**, *13*, 6576–6579.

[9] a) R. K. Haynes, T.-L. Au-Yeung, W.-K. Chan, W.-L. Lam, Z.-Y. Li, L.-L. Yeung, A. S. C. Chan, P. Li, M. Koen, C. R. Mitchell, et al., *Eur. J. Org. Chem.* **2000**, 3205–3216; b) Q. Xu, C.-Q. Zhao, L.-B. Han, *J. Am. Chem. Soc.* **2008**, *130*, 12648–12655; c) A. J. Bloomfield, S. B. Herzon, *Org. Lett.* **2012**, *14*, 4370–4373; d) S.-Z. Nie, Z.-Y. Zhou, J.-P. Wang, H. Yan, J.-H. Wen, J.-J. Ye, Y.-Y. Cui, C.-Q. Zhao, *J. Org. Chem.* **2017**, *82*, 9425–9434; e) Z. S. Han, H. Wu, Y. Xu, Y. Zhang, B. Qu, Z. Li, D. R. Caldwell, K. R. Fandrick, L. Zhang, F. Roschangar, et al., *Org. Lett.* **2017**, *19*, 1796–1799; f) J. Chrzanowski, D. Krasowska, M. Urbaniak, L. Sieroń, P. Pokora-Sobczak, O. M. Demchuk, J. Drabowicz, *Eur. J. Org. Chem.* **2018**, 4614–4627.

[10] a) P. Kiełbasiński, R. Żurawiński, K. M. Pietrusiewicz, M. Zabłocka, M. Mikołajczyk, *Tetrahedron Lett.* **1994**, *35*, 7081–7084; b) K. Shioji, Y. Ueno, Y. Kurauchi, K. Okuma, *Tetrahedron Lett.* **2001**, *42*, 6569–6571; c) S. Kaczmarczyk, M. Kwiatkowska, L. Madalińska, A. Barbachowska, M. Rachwalski, J. Błaszczyk, L. Sieroń, P. Kiełbasiński, *Adv. Synth. Catal.* **2011**, *353*, 2446–2454; d) Y. Zhang, H. He, Q. Wang, Q. Cai, *Tetrahedron Lett.* **2016**, *57*, 5308–5311; e) H. Fernández-Pérez, A. Vidal-Ferran, *Org. Lett.* **2019**, *21*, 7019–7023.

[11] a) E. Bergin, C. T. O'Connor, S. B. Robinson, E. M. McGarrigle, C. P. O'Mahony, D. G. Gilheany, *J. Am. Chem. Soc.* **2007**, *129*, 9566–9567; b) K. V. Rajendran, L. Kennedy, D. G. Gilheany, *Eur. J. Org. Chem.* **2010**, 5642–5649; c) K. Nikitin, K. V. Rajendran, H. Müller-Bunz, D. G. Gilheany, *Angew. Chem. Int. Ed.* **2014**, *53*, 1906–1909; *Angew. Chem.* **2014**, *126*, 1937; d) K. V. Rajendran, K. V. Nikitin, D. G. Gilheany, *J. Am. Chem. Soc.* **2015**, *137*, 9375–9381; e) K. M.-H. Lim, T. Hayashi, *J. Am. Chem. Soc.* **2017**, *139*, 8122–8125; f) A. Ironmonger, M. Shipton, F. Slater, P. Szeto, M. G. Unthank, F. R. Alexandre, C. Caillet, C. B. Dousson, *Tetrahedron Lett.* **2018**, *59*, 2154–2156; g) A. Mohd, T. Anitha, K. R. Reddy, J. Wencel-Delord, F. Colobert, *Eur. J. Org. Chem.* **2019**, 7836–7841.

[12] a) F. Toda, K. Mori, S. Zafra, I. Goldberg, *J. Org. Chem.* **1988**, *53*, 308–312; b) J. Drabowicz, P. Łyżwa, J. Omelańczuk, K. M. Pietrusiewicz, M. Mikołajczyk, *Tetrahedron: Asymmetry* **1999**, *10*, 2757–2763; c) J. Holt, A. M. Maj, E. P. Schudde, K. M. Pietrusiewicz, L. Sieroń, W. Wieczorek, T. Jerphagnon, I. W. C. E. Arends, U. Hanefeld, A. J. Minnaard, *Synthesis* **2009**, 2061–2065; d) F. A. Kortmann, M.-C. Chang, E. Otten, E. P. A. Couzijn, M. Lutz, A. J. Minnaard, *Chem. Sci.* **2014**, *5*, 1322–1327; e) P. Bagi, V. Ujj, M. Czugler, E. Fogassy, G. Keglevich, *Dalton Trans.* **2016**, *45*, 1823–1842; f) P. Bagi, B. Varga, A. Szilágyi, K. Karaghiosoff, M. Czugler, E. Fogassy, G. Keglevich, *Chirality* **2018**, *30*, 509–522.

[13] G. Li, X. Wang, Y. Zhang, Z. Tan, P. DeCroos, J. C. Lorenz, X. Wei, N. Grinberg, N. K. Yee, C. H. Senanayake, *J. Org. Chem.* **2017**, *82*, 5456–5460.

[14] a) F. Faigl, E. Fogassy, M. Nógrádi, E. Pálovics, J. Schindler, *Tetrahedron: Asymmetry* **2008**, *19*, 519–536; b) H. Lorenz, A. Seidel-Morgenstern, *Angew. Chem. Int. Ed.* **2014**, *53*, 1218–1250; *Angew. Chem.* **2014**, *126*, 1240; c) S. Mane, *Anal. Methods* **2016**, *8*, 7567–7586.

[15] a) D. Seebach, A. K. Beck, A. Heckel, *Angew. Chem. Int. Ed.* **2001**, *40*, 92–138; *Angew. Chem.* **2001**, *113*, 96; b) H. Pellissier, *Tetrahedron* **2008**, *64*, 10279–10317; c) K. Tanaka in *Comprehensive Chirality Vol. 8* (Eds.: E. M. Carreira, H. Yamamoto), Elsevier, Amsterdam, **2012** pp. 63–90; d) B. Yang, H. Xie, K. Ran, Y. Gan, *Lett. Org. Chem.* **2017**, *15*, 10–14.

[16] P. Bagi, R. Herbay, in *Organophosphorus Chemistry - Novel Developments* (Ed.: G. Keglevich), De Gruyter, Berlin, **2018**, pp. 66–90.

[17] J. Meisenheimer, J. Casper, M. Höring, W. Lauter, L. Lichtenstadt, W. Samuel, *Justus Liebigs Ann. Chem.* **1926**, *449*, 213–248.

[18] G. Szekely, M. F. Jimenez-Solomon, P. Marchetti, J. F. Kim, A. G. Livingston, *Green Chem.* **2014**, *16*, 4440–4473.

[19] a) N. F. Ghazali, F. C. Ferreira, A. J. P. White, A. G. Livingston, *Tetrahedron: Asymmetry* **2006**, *17*, 1846–1852; b) N. F. Ghazali, F. C. Ferreira, A. J. P. White, A. G. Livingston, *Desalination* **2006**, *199*, 398–400; c) I. Sereewatthanawut, F. C. Ferreira, N. F. Ghazali, A. G. Livingston, *AIChE J.* **2010**, *56*, 893–904.

[20] C. Didaskalou, J. Kupai, L. Cseri, J. Barabas, E. Vass, T. Holtzl, G. Szekely, *ACS Catal.* **2018**, *8*, 7430–7438.

[21] P. Kisszekelyi, A. Alammar, J. Kupai, P. Huszthy, J. Barabas, T. Holtzl, L. Szente, C. Bawn, R. Adams, G. Szekely, *J. Catal.* **2019**, *371*, 255–261.

[22] B. Zupančič, B. Mohar, M. Stephan, *Adv. Synth. Catal.* **2008**, *350*, 2024–2032.

[23] K. M. Pietrusiewicz, M. Zablocka, J. Monkiewicz, *J. Org. Chem.* **1984**, *49*, 1522–1526.

[24] a) K. Matsumoto, T. Okamoto, K. Otsuka, *Bull. Chem. Soc. Jpn.* **2004**, *77*, 2051–2056; b) K. Matsumoto, K. Otsuka, T. Okamoto, H. Mogi, *Synlett* **2007**, 729–732.

[25] a) H. Kaku, A. Nakamaru, M. Inai, T. Nishii, M. Horikawa, T. Tsunoda, *Tetrahedron* **2010**, *66*, 9450–9455; b) H. Kaku, T. Imai, R. Kondo, S. Mamba, Y. Watanabe, M. Inai, T. Nishii, M. Horikawa, T. Tsunoda, *Eur. J. Org. Chem.* **2013**, 8208–8213; c) H. Kaku, M. Ito, M. Horikawa, T. Tsunoda, *Tetrahedron* **2018**, *74*, 124–129.

[26] P. Bagi, A. Fekete, M. Kállay, D. Hessz, M. Kubinyi, T. Holczbauer, M. Czugler, E. Fogassy, G. Keglevich, *Heteroat. Chem.* **2015**, *26*, 79–90.

[27] a) M. A. Spackman, D. Jayatilaka, *CrystEngComm* **2009**, *11*, 19–32; b) S. P. Thomas, P. R. Spackman, D. Jayatilaka, M. A. Spackman, *J. Chem. Theory Comput.* **2018**, *14*, 1614–1623.

[28] a) R. K. Henderson, C. Jiménez-González, D. J. C. Constable, S. R. Alston, G. G. A. Inglis, G. Fisher, J. Sherwood, S. P. Binks, A. D. Curzons, *Green Chem.* **2011**, *13*, 854; b) F. P. Byrne, S. Jin, G. Paggiola, T. H. M. Petchey, J. H. Clark, T. J. Farmer, A. J. Hunt, C. R. McElroy, J. Sherwood, *Sustainable Chem. Process.* **2016**, *4*, 7.

[29] G. Székely, J. Bandarra, W. Heggie, B. Sellergren, F. C. Ferreira, *J. Membr. Sci.* **2011**, *381*, 21–33.

Received: January 10, 2020